Research Paper

Metal-linked Immunosorbent Assay (MeLISA): the Enzyme-Free Alternative to ELISA for Biomarker Detection in Serum

Ru-Jia Yu[1][†], Wei Ma[1][†], Xiao-Yuan Liu[1], Hong-Ying Jin[1], Huan-Xing Han[2], Hong-Yang Wang[3], He Tian[1][✉], Yi-Tao Long[1][✉]

1. Key Laboratory for Advanced Materials, School of Chemistry & Molecular Engineering, East China University of Science and Technology, P. R. China.
2. Translational Medicine Center, Changzheng Hospital, The Second Military Medical University, P. R. China.
3. Laboratory of Signal Transduction, Eastern Hepatobiliary Surgery Hospital, The Second Military Medical University, P. R. China.

†These authors contributed equally.

✉ Corresponding authors: H.T. (tianhe@ecust.edu.cn) or Y.T.L. (ytlong@ecust.edu.cn)

Abstract

Determination of disease biomarkers in clinical samples is of crucial significance for disease monitoring and public health. The dominating format is enzyme-linked immunosorbent assay (ELISA), which subtly exploits both the antigen-antibody reaction and biocatalytic property of enzymes. Although enzymes play an important role in this platform, they generally suffer from inferior stability and less tolerant of temperature, pH condition compared with general chemical product. Here, we demonstrate a metal-linked immunosorbent assay (MeLISA) based on a robust signal amplification mechanism that faithfully replaces the essential element of the enzyme. As an enzyme-free alternative to ELISA, this methodology works by the detection of α-fetoprotein (AFP), prostatic specific antigen (PSA) and C-reactive protein (CRP) at concentrations of 0.1 ng mL^{-1}, 0.1 ng mL^{-1} and 1 ng mL^{-1} respectively. It exhibits approximately two magnitudes higher sensitivity and is 4 times faster for chromogenic reaction than ELISA. The detection of AFP and PSA was further confirmed by over a hundred serum samples from hepatocellular carcinoma (HCC) and prostate cancer patients respectively.

Key words: MeLISA

Introduction

Enzyme-free detection is extremely desirable [1–3] yet still challenging to the engineering of robust methods which would renovate immunoassay and improve current diagnostic techniques. Although extensive research has been devoted including the use of electrochemistry [4–6], fluorescence [7,8] and chemiluminescence [9–11], the requirement of additional expensive equipment discourages their broad application especially in resource limited regions. Since the color generation is the basis of ELISA, engineering enzyme-free colorimetric assay could not only well accommodate conventional immunoassay, but also greatly improve its stability.

The development of nanotechnology opens the way for advances in scientific research [12–18]. With the synthetic procedure towards nanoparticles having been optimized, biosensors based on nanomaterials are moving into clinical practice and commercial translation [19]. Conventional gold nanoparticles (AuNPs)-based colorimetric detection yields high sensitivity due to the high extinction coefficient and distance-dependent optical properties [20–25], nonetheless, current AuNPs aggregation induced by interparticle crosslinking of biomolecules often requires careful and long-time incubation in a buffer solution which may cause undesirable aggregation of

AuNPs [26]. Robust, ultra-rapid and highly stable AuNPs aggregation in colorimetric assay still remains a challenge. We circumvent this problem by presenting an organic reaction-induced aggregation in aqueous solution which occurs within 1 second. This aggregation of AuNPs is triggered by the reaction between terminal alkynes and silver ions, which has been used as a "traditional test" for acetylenic groups (depicted in Fig. 1). We adopt this classic reaction for the first time in a colorimetric assay. Surprisingly, it yielded the fastest AuNPs-based colorimetric process ever reported (Table S1).

Herein, this colorimetric assay was integrated into immunoassay by employing the silver ions generation amplification. In our approach, silver nanoparticles (AgNPs) were oxidatively dissolved in the presence of hydrogen peroxide to produce millions of silver ions. Instead of the standard enzymatic reaction under well-defined conditions in an ELISA test, the robust chemical dissolution and the ultra-rapid colorimetric process ensure a high reproducible and practical system. The amplification mechanism exhibits attractive size-modulation, that is, AgNPs with differing diameters generate silver ions of corresponding amounts, leading to a controlled detecting range of analyte. That is of vital importance for an analytical methodology since the reference ranges for different analytes varies significantly. The MeLISA offers a simple but effective platform for biomarker detection with high stability and robustness.

Alkynyl silvers induced colorimetric assay

The formation of alkynyl silvers has wide applications in organic synthesis [27,28], silver-catalyzed reaction [29,30] and building blocks for complex architectures [31,32]. To employ this organic reaction for colorimetric assay, terminal alkyne-functionalized thiol (5-(1,2-dithiolan-3-yl)-N-(prop-2-ynyl) pentanamide) was synthesized following previously reported methodology [33]. This compound was spontaneously self-assembled onto the surface of AuNPs through Au-S bonds which could be confirmed by a slight red shift in the UV-Vis spectra (Fig. S1). By introducing silver ions to the alkyne-functionalized AuNPs, the H of the C-H bond of the alkyne was exchanged by the silver (I) species, immediately forming alkynyl silvers complex. Fig. 2a shows the different tonality of the alkyne-functionalized AuNPs solution upon treatment with different concentrations of silver nitrate; the colour intensity increased at higher concentrations of silver ions, and the colour remained fixed overnight. The blue coloured solutions were characterized by the UV-Vis spectra as demonstrated in Fig. 2b. At higher concentration of silver ions, the absorbance at 620 nm ($A_{620\,nm}$) was intensified, which was related to aggregation of AuNPs, whereas the extinction at 520 nm (A_{520nm}), corresponding to dispersed AuNPs, was decreased. The absorbance ratio between $A_{620\,nm}$ and $A_{520\,nm}$ was proportional to the concentration of silver ions below 10 µM (Fig. 2c), indicating that this colorimetric assay was potentially quantifiable.
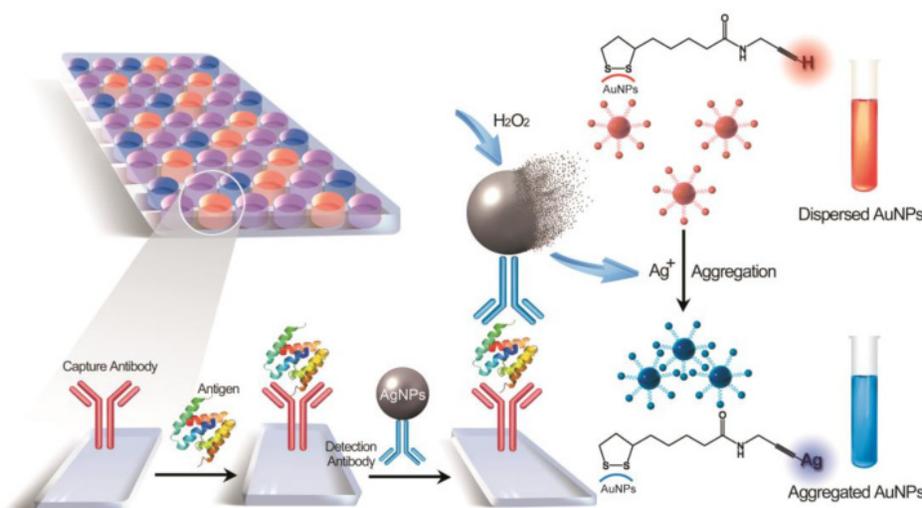

Figure 1. Schematic representation of the MeLISA for the detection of biomarker. In this sandwich immunoassay, the polystyrene plate is covered with a capture antibody which could anchor the target biomarker. This coating step comprises the blocking procedure with bovine serum albumin to minimize nonspecific interactions. Serum sample with target antigen is added to the plate to allow the reaction between capture antibody and target antigen. Finally, the sandwich immunoassay is formed by the addition of the detection antibody that conjugated with silver nanoparticles. Introduction of hydrogen peroxide initiates the dissolution of AgNPs into silver ions, leading to a rapid aggregation of alkyne-functionalized AuNPs. The aggregation yields a distinct red-to-blue colour change in solution that can be read by eye or a compatible plate reader (for quantification).
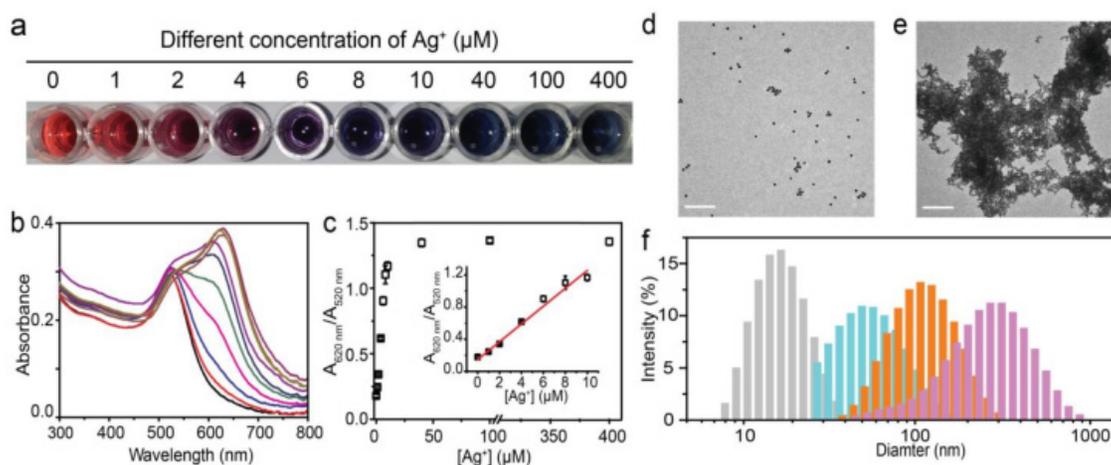
Figure 2. The aggregation of alkyne-functionalized AuNPs induced by silver ions. a, Visual colour distribution upon treatment of the alkyne-functionalized AuNPs system with various concentrations of Ag^+ range from 1 to 400 µM. The photograph was taken less than three seconds after the addition of Ag^+. **b,** UV-Vis spectra of the alkyne-functionalized AuNPs system in the presence of Ag^+ with concentrations from 1 to 400 µM. The absorbance at 620 nm indicates the aggregation of alkyne-functionalized AuNPs. **c,** Plot of $A_{620\,nm}/A_{520\,nm}$ against different concentrations of Ag^+. The inset is a linear relationship at low concentration of Ag^+. Error bars are based on three independent measurements. **d, e,** Transmission electron microscopy (TEM) images of the dispersed and aggregated alkyne-functionalize AuNPs in the absence (d) and presence (e) of Ag^+. Scale bar: 200 nm. **f,** DLS analysis of alkyne-functionalized AuNPs in the presence of 0 µM (gray), 4 µM (blue), 8 µM (orange), 40 µM (purple) silver ions.

The aggregation was due to the formation of alkynyl silvers which could change the surface charge of alkyne-functionalized AuNPs. The high efficient nature of this organic reaction, results in a fast aggregation within 1 second at room temperature. This is the most rapid AuNPs-based colorimetric process ever reported. The aggregation of alkyne-functionalized AuNPs could be directly confirmed by transmission electron microscopy (TEM) images. It clearly displayed a dispersed or aggregated state of alkyne-functionalized AuNPs in the absence or presence of silver ions, respectively (Fig. 2d, e). Dynamic light scattering (DLS) was also employed to validate the aggregation. The diameter of alkyne-functionalized AuNPs enlarges gradually with the addition of higher concentration of silver ions (Fig. 2f).

To confirm that the aggregation was actually induced by the reaction between the terminal alkyne and silver ions, bare AuNPs were challenged with different concentrations of silver ions in the same conditions; the solutions remained unchanged (Fig. S2). In addition, silver ions were replaced by other metal ions in the presence of alkyne-functionalized AuNPs, including K^+, Na^+, Ca^{2+}, Fe^{2+}, Cu^{2+}, Pd^{2+}, Zn^{2+} and Mn^{2+}. Even at a concentration ten times greater than that of silver ions and with the solution standing overnight, no colour change was observed in solution (Fig. S3). Therefore the aggregation in our method was triggered by the organic reaction between terminal alkynes and silver ions. Although Cu (I) may have the same function as silver ions due to the same reaction with terminal alkynes (data not shown), the effect can be neglected because of the instability of this compound. Taken together, the aggregation of alkyne-functionalized AuNPs induced by silver ions can be used in colorimetric assay due to the rapid response, high stability and capability to produce an intense optical response.

MeLISA for biomarker detection

We used the dissolution of AgNPs for signal amplification, taking the place of enzymatic process. When H_2O_2 was added to the 70-nm AgNPs (see Fig. S4 for UV-Vis and TEM characterization), the solution began to fade and became colourless, indicating a resultant dissolution of AgNPs [34]. The dissolution was evaluated by UV-Vis spectra and dark field imaging. As depicted in Fig. S5, the absorbance at 420 nm, which is a characteristic absorbance peak for AgNPs, decreased significantly and eventually disappeared within a few minutes after the addition of H_2O_2. Meanwhile, blue spots of AgNPs in the dark field microscope image gradually disappeared after incubation with H_2O_2 (Fig. S6). Compared with the dissolution with strong acid [35], H_2O_2 offers a relatively mild and environment-friendly methodology and makes a minimal contribution to AuNPs aggregation. Moreover, the dissolution of AgNPs enables a great amplification: it can be calculated that each 70 nm AgNPs would generate silver ions by seven orders of magnitude through the dissolution. To employ this amplification into biomarker detection, we used an AgNPs-linked antibody to accommodate a sandwich immunoassay and establish the MeLISA system (the combination of antibody to AgNPs was described in supporting information).
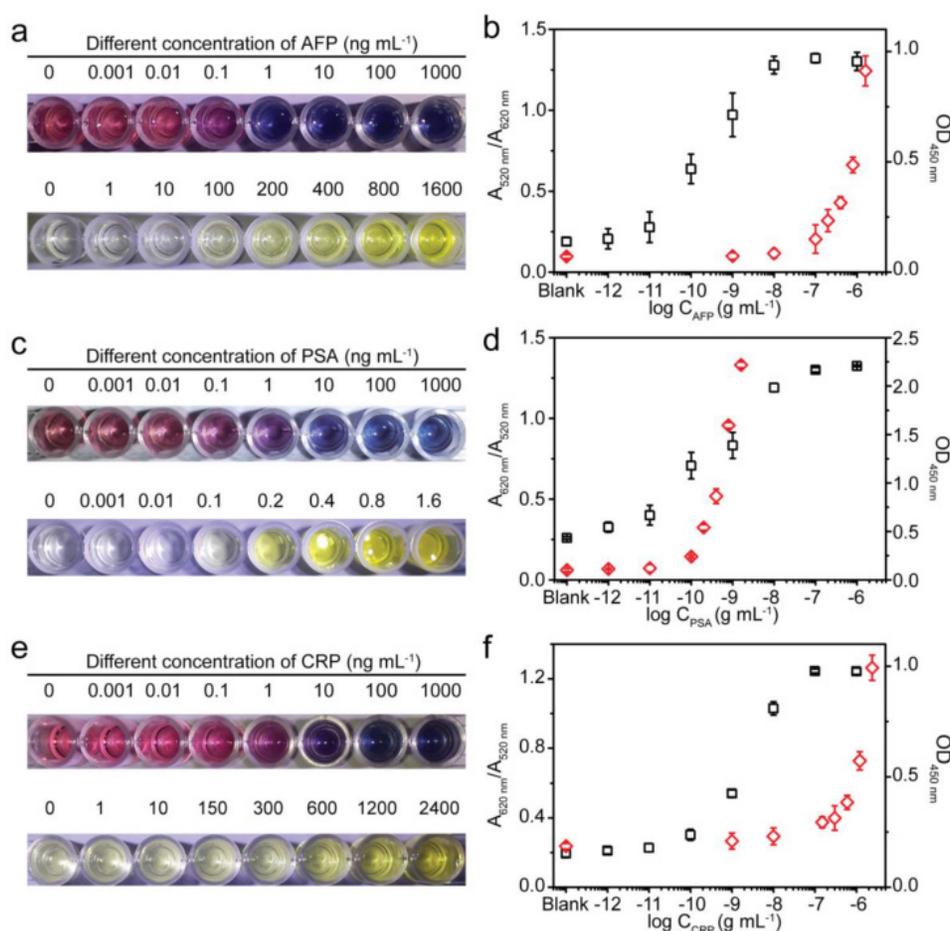
Figure 3. A comparison between the MeLISA and conventional ELISA for biomarker detection. a, Photographs showing the performance for AFP detection using the MeLISA and commercial ELISA kit. **b,** Values of corresponding peak absorbance versus different AFP concentrations. The black squares represent the value of $A_{620\,nm}/A_{520\,nm}$ obtained through the MeLISA and red diamonds represent the value of $OD_{450\,nm}$ obtained through conventional ELISA. **c,** The detection of PSA using our MeLISA and ELISA. **d,** Values of corresponding peak absorbance versus different PSA concentrations. **e,** The detection of CRP using MeLISA and ELISA. **f,** Values of corresponding peak absorbance versus different CRP concentrations. Error bars are based on three independent measurements.

We used the MeLISA for the colorimetric detection of AFP, a valuable biomarker for hepatocellular carcinoma (HCC). Briefly, a polystyrene plate modified with capture antibody was exposed to 1% bovine serum albumin (BSA) to block the remaining protein binding sites. After repeated washing, target antigen was added to the desired concentration and the blank was run to ensure the accuracy, followed by another washing. The plate was then incubated with AgNPs-AB (the AgNPs labelled antibody denoted as AgNPs-AB, the incubation time and concentration of antibody were optimized as shown in Fig. S7, 8). Another washing step was performed and subsequently H_2O_2 and alkyne-functionalized AuNPs were added successively to generate the colour change in solution. With the addition of H_2O_2, AgNP-AB was dissolved into silver ions which induced the aggregation of alkyne-functionalized AuNPs. The solution exhibited blue colour only in the presence of AFP, and higher concentrations of analyte favoured a high intensity

blue colour in the solution (Fig. 3a). In the blank control, no silver ions were generated to induce the AuNPs aggregation because AgNPs-AB could not be adsorbed to the wells without the recognition by the target analyte. Conventional HRP-based ELISA was performed as comparison according to a standard protocol. As shown in Fig. 3a, an AFP concentration as low as 10^{-10} g mL^{-1} could be detected by the distinct colour difference in solution using our MeLISA, whereas it needed nearly a concentration of 10^{-7} g mL^{-1} for colorimetric differentiation in conventional ELISA. The colorimetric detection ability of MeLISA could be validated by the ratio between the absorbance at 620 nm and 520 nm ($A_{620\,nm}/A_{520\,nm}$, see Fig. S9 for the corresponding UV-Vis spectra). Likewise, the optical density at 450 nm ($OD_{450\,nm}$) could be used to verify the colorimetric results of ELISA (Fig. 3b). These results represent a nearly 1000-fold decrease in the limit of detection compared with conventional ELISA, and the high sensitivity was promoted by the unique signal amplification in the

MeLISA system. On the one hand, the colour change of functionalized AuNPs is sensitive to silver ions on which the assay is based. Through this particle-to-ions amplification, a low concentration of silver nanoparticles could produce an obvious blue-coloured solution. On the other hand, through the metal-linked amplification, each 70-nm AgNP would generate millions of silver ions through dissolution, resulting in a significant enhancement in biomarker detection. Besides the higher sensitivity, the MeLISA has advantages over ELISA. As biological signal amplification in ELISA, the enzymatic process should under well-defined conditions, require approximately 20 minutes and need to be stopped by inactivating the enzymes. Furthermore, in ELISA, the colorimetric results produced by chromogenic reagent were not stable and the results of $OD_{450 \, nm}$ should be measured within 15 min in case the decrease of the optical density. By contrast, in the MeLISA system, robust chemical reaction was introduced for signal amplification. That required only 5-6 minutes and no special reaction conditions (e.g. dark conditions, precise pH, constant temperature and buffer solution that should be ensured in ELISA) were needed. For the organic reaction-induced aggregation of AuNPs, the colorimetric results were stable and the absorbance could be measured even overnight using an identical microplate reader. The assay performance could certainly be improved by using secondary antibody or using biotin streptavidin amplification system like the ELISA does. Therefore, this MeLISA platform offered a suitable enzyme-free alternative to conventional ELISA, especially in resource-limited environment.

To test the ability of the MeLISA as a universal tool for antigen detection, we also evaluated the detection of prostate specific antigen (PSA) and C-reactive protein (CRP), pivotal biomarkers for prostate cancer and human inflammation respectively. Identical to the AFP detection described above, anti-PSA and anti-CRP were used to produce sandwich immunoassays. The solution exhibited a blue (yellow) colour only in the presence of target analyte which was due to the selectivity of antigen-antibody reaction. For PSA, with low concentration even in patients, our MeLISA could obtain a comparable detection limit with conventional ELISA which was 10^{-10} g mL^{-1}. Additionally, MeLISA offered a wider detection range (Fig. 3c). The detection performance could also be confirmed by the values of $A_{620 \, nm}/A_{520 \, nm}$ and $OD_{450 \, nm}$ (Fig. 3d). For CRP, a concentration of 10^{-9} g mL^{-1} could be discriminated through the red-to-blue colour difference in MeLISA, indicating approximately two orders of magnitude higher sensitivity than that for

conventional ELISA (Fig. 3e,f) More importantly, CRP is a high-content protein even in normal subjects and µg mL^{-1} concentration in patients. We could achieve direct colorimetric readout by adjusting the size of the AgNPs to avoid repeated dilution in traditional sensitive detection methods. The detecting range of analyte could be controlled beforehand due to the AgNPs-to-Ag$^+$ amplification. Fig. S10 shows that the concentration of CRP only in the range of 10^{-9}-10^{-7} g mL^{-1} could be differentiated using 70 nm AgNPs. While by using 15 nm AgNPs, the CRP concentration in the range of 10^{-7}-10^{-6} g mL^{-1} could then be distinguished (see Fig. S11 for UV-Vis and TEM characterization). By changing the size of AgNPs, the detection range of our MeLISA system could be directly regulated according to different threshold concentrations for different biomarkers. Overall, we believe that the MeLISA could be a suitable replacement for enzymatic ELISA approach as a universal method for biomarker detection.

Real sample detection of AFP by the MeLISA

Many detection methods failed to monitor target antigen in clinical samples, which is more complex and often in low concentration. Encouraged by the sensitivity and robustness of the MeLISA, we evaluated the MeLISA system under clinical diagnostic conditions. To ensure the reliability and objectivity, a double-blind experiment was performed using 96 unrelated serum samples with a 100-fold dilution (52 AFP positive samples were collected from HCC patients and 44 negative ones were from healthy people. The experimenter did not know the concentrations of these samples until the experiment was finished). As demonstrated in Fig. 4a, positive and negative samples could be differentiated by the colour of the resulting solution with aggregated or dispersed AuNPs respectively. The value of $A_{620 \, nm}/A_{520 \, nm}$ could also be used to distinguish the samples with a clinical threshold of 20 ng mL^{-1} where the $A_{620 \, nm}/A_{520 \, nm}$ value was 0.31, positive samples yielded higher $A_{620 \, nm}/A_{520 \, nm}$ values while negative samples yielded lower ones (Fig. 4b). 5 samples produced false-negative results among a total 96 samples, indicating that the MeLISA offered sensitivity of 90% and specificity of 100% in one independent experiment. The area under ROC curve (AUC) was calculated to be 0.96, indicating excellent discrimination of our MeLISA (Fig. 4c, see Table S2 for raw data). The excellent performance verified the ability of our MeLISA to perform AFP detection using small volumes of serum to produce a distinct colorimetric result. Furthermore, to demonstrate the practical application of the MeLISA, user friendliness

should be considered. A novice was asked to perform the experiment from beginning to end including the synthesis of alkyne-functionalized AuNPs, the label of antibody to AgNPs and the immunosorbent assay. With 32 serum samples, 100% sensitivity and 82% specificity were obtained in one independent assay and the AUC was 0.96 as depicted in Fig. S12. The MeLISA could be adjusted to a clinical diagnostic of HCC by the high performance in AFP detection.

Real sample detection of PSA by the MeLISA

To test the universality of the MeLISA for detecting different biomarkers in sera, PSA was used to evaluate the performance using 30 serum samples with 15 positive. With a 10-fold dilution, Fig. 5a demonstrated the colorimetric results in a double-blind experiment. At the clinical threshold of 4 ng mL^{-1}, 0.38 was used as $A_{620 nm}/A_{520 nm}$ cut-off value to differ positive and negative samples (Fig. 5b). All the samples were accurately detected indicating that the sensitivity and selectivity, for PSA detection, were both 100% which rival the existing methods (Fig. 5c, see Table S3 for raw data). To ensure the reproducibility of the MeLISA, coefficient of variation (CV) was obtained through three independent assays. CV% was under 15% in 28 cases which demonstrated the high reproducibility and accuracy of our method

(Fig. 5d). Overall, the MeLISA was able to detect any other disease biomarkers as long as the antibody direct against it are available like ELISA. Given the significant advantages of simple, stable and reliable features, the MeLISA could indeed be a suitable replacement to ELISA in clinical diagnostic. It could potentially be developed to a commercial kit like ELISA since nanoparticles (both silver and gold) could be easily obtained at a low cost.

In conclusion, we have demonstrated an enzyme-free methodology for the colorimetric detection of disease biomarkers in serum which could be used in clinical diagnostic. Our metal-linked amplification strategy was efficient and robust by the chemical dissolution of AgNPs into silver ions; a "well-known test" for acetylenic groups was used to develop a colorimetric immunoassay which generates a high signal response. In view of the results for the detection of various biomarkers and the excellent performance in clinical evaluation, the MeLISA could represent an enzyme-free alternative to conventional ELISA, especially in point-of-care diagnostics. Since the colorimetric assays can be used for the detection of proteins and also small molecules, our approach may be capable of accommodating many biological problems and as such could potentially afford substantial impact in the development of novel analytical methods.
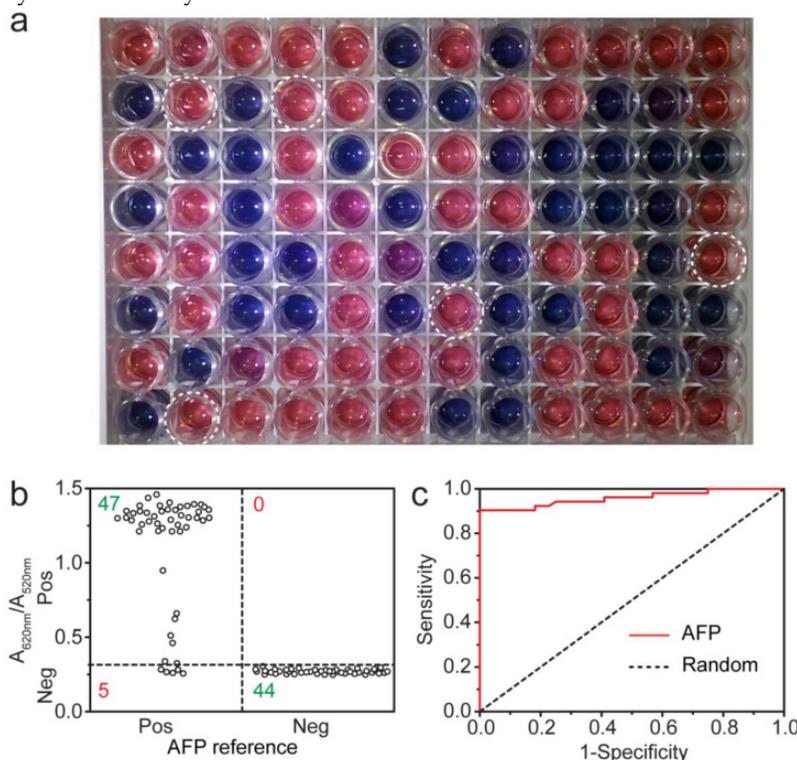

Figure 4. Colorimetric detection of AFP in human serum by the MeLISA. A double-blind experiment was performed for the detection of AFP in serum from clinical patients. **a,** Photograph for the AFP detection in 96 unrelated real samples using the MeLISA. Negative samples yielded red solution with dispersed AuNPs, whereas positive ones yielded blue or purple solution with aggregated AuNPs. 5 false-negative samples were marked with white circle. **b,** Vertical scatter plots of the values of $A_{620 nm}/A_{520 nm}$ for positive and negative samples (each serum sample is represented by one solid circle for AFP detection). **c,** Receiver operating characteristic (ROC) curve was employed to illustrate the sensitivity and specificity of the MeLISA for AFP in clinical samples.
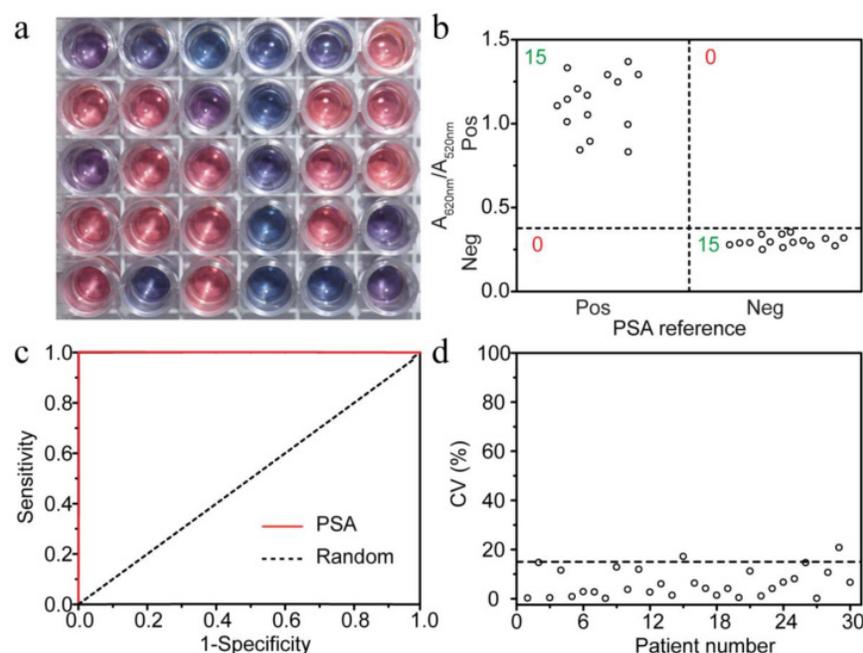
Figure 5 | Colorimetric detection of PSA in human serum by the MeLISA. A double-blind experiment was performed for PSA detection in serum samples. **a,** Photograph for the detection in 30 independent real samples using the MeLISA. **b,** Vertical scatter plots of the values of $A_{620\,nm}/A_{520\,nm}$ for positive and negative samples. **c,** ROC curve for PSA in clinical samples. **d,** Coefficient of variation (CV) plotted with different patient numbers. The CV was obtained through three independent experiments and the marked cut-off was 15%.

Supplementary Material

Supplementary information and figures.
http://www.thno.org/v06p1732s1.pdf

Acknowledgements

Competing Interests

The authors have declared that no competing interest exists.

References

1. Zhao W-W, Han Y-M, Zhu Y-C, Zhang N, Xu J-J, Chen H-Y. DNA Labeling Generates a Unique Amplification Probe for Sensitive Photoelectrochemical Immunoassay of HIV-1 p24 Antigen. Anal Chem. 2015; 87:5496–5499.
2. Zheng A-X, Li J, Wang J-R, Song X-R, Chen G-N, Yang H-H. Enzyme-free signal amplification in the DNAzyme sensor via target-catalyzed hairpin assembly. Chem Commun. 2012; 48:3112.
3. Tian D, Duan C, Wang W, Cui H. Ultrasensitive electrochemiluminescence immunosensor based on luminol functionalized gold nanoparticle labeling. Biosens Bioelectron. 2010; 25:2290–2295.
4. Yu X, Munge B, Patel V, et al. Carbon nanotube amplification strategies for highly sensitive immunodetection of cancer biomarkers. J Am Chem Soc. 2006; 128:11199–11205.
5. Akanda MR, Aziz MA, Jo K, et al. Optimization of Phosphatase- and Redox Cycling-Based Immunosensors and Its Application to Ultrasensitive Detection of Troponin I. Anal Chem. 2011; 83:3926–3933.
6. Lai G, Yan F, Wu J, Leng C, Ju H. Ultrasensitive Multiplexed Immunoassay with Electrochemical Stripping Analysis of Silver Nanoparticles Catalytically Deposited by Gold Nanoparticles and Enzymatic Reaction. Anal Chem. 2011; 83:2726–2732.
7. Chan WC, Nie S. Quantum dot bioconjugates for ultrasensitive nonisotopic detection. Science. 1998; 281:2016–2018.
8. Rissin DM, Kan CW, Campbell TG, et al. Single-molecule enzyme-linked immunosorbent assay detects serum proteins at subfemtomolar concentrations. Nat Biotechnol. 2010; 28:595–599.
9. Deiss F, LaFratta CN, Symer M, Blicharz TM, Sojic N, Walt DR. Multiplexed sandwich immunoassays using electrochemiluminescence imaging resolved at the single bead level. J Am Chem Soc. 2009; 131:6088–6089.
10. Lin D, Wu J, Yan F, Deng S, Ju H. Ultrasensitive immunoassay of protein biomarker based on electrochemiluminescent quenching of quantum dots by hemin bio-bar-coded nanoparticle tags. Anal Chem. 2011; 83:5214–5221.
11. Xu S, Liu Y, Wang T, Li J. Positive potential operation of a cathodic electrogenerated chemiluminescence immunosensor based on luminol and graphene for cancer biomarker detection. Anal Chem. 2011; 83:3817–3823.
12. Choi Y, Park Y, Kang T, Lee LP. Selective and sensitive detection of metal ions by plasmonic resonance energy transfer-based nanospectroscopy. Nat Nanotechnol. 2009; 4:742–746.
13. Ma W, Kuang H, Xu L, et al. Attomolar DNA detection with chiral nanorod assemblies. Nat Commun. 2013; 4:2689.
14. De la Rica R, Stevens MM. Plasmonic ELISA for the ultrasensitive detection of disease biomarkers with the naked eye. Nat Nanotechnol. 2012; 7:821–824.
15. Rodríguez-Lorenzo L, de la Rica R, Álvarez-Puebla R a., Liz-Marzán LM, Stevens MM. Plasmonic nanosensors with inverse sensitivity by means of enzyme-guided crystal growth. Nat Mater. 2012; 11:604–607.
16. Shen Y, Zhou J, Liu T, et al. Plasmonic gold mushroom arrays with refractive index sensing figures of merit approaching the theoretical limit. Nat Commun. 2013; 4:2381.
17. Kosaka PM, Pini V, Ruz JJ, et al. Detection of cancer biomarkers in serum using a hybrid mechanical and optoplasmonic nanosensor. Nat Nanotechnol. 2014; 9:1047–53.
18. Peng M-P, Ma W, Long Y-T. Alcohol Dehydrogenase-Catalyzed Gold Nanoparticle Seed-Mediated Growth Allows Reliable Detection of Disease Biomarkers with the Naked Eye. Anal Chem. 2015; 87:5891–5896.
19. Howes PD, Chandrawati R, Stevens MM. Colloidal nanoparticles as advanced biological sensors. Science 2014; 346:1247390–1247390.
20. Lu C-H, Wang Y-W, Ye S-L, Chen G-N, Yang H-H. Ultrasensitive detection of Cu2+ with the naked eye and application in immunoassays. NPG Asia Mater. 2012; 4:e10.
21. Qu W, Liu Y, Liu D, Wang Z, Jiang X. Copper-mediated amplification allows readout of immunoassays by the naked eye. Angew Chem Int Ed. 2011; 50:3442–3445.
22. Liu D, Yang J, Wang HF, et al. Glucose oxidase-catalyzed growth of gold nanoparticles enables quantitative detection of attomolar cancer biomarkers. Anal Chem. 2014; 86:5800–5806.
23. Liu D, Wang Z, Jin A, et al. Acetylcholinesterase-catalyzed hydrolysis allows ultrasensitive detection of pathogens with the naked eye. Angew Chem Int Ed. 2013; 52:14065–14069.

24. Elghanian R, Storhoff JJ, Mucic RC, Letsinger RL, Mirkin C a. Selective colorimetric detection of polynucleotides based on the distance-dependent optical properties of gold nanoparticles. Science. 1997; 277:1078–1081.

25. Lee JS, Han MS, Mirkin C a. Colorimetric detection of mercuric ion (Hg2+) in aqueous media using DNA-functionalized gold nanoparticles. Angew Chem Int Ed. 2007; 46:4093–4096.

26. Zhang M, Qing G, Xiong C, Cui R, Pang DW, Sun T. Dual-responsive gold nanoparticles for colorimetric recognition and testing of carbohydrates with a dispersion-dominated chromogenic process. Adv Mater. 2013; 25:749–754.

27. Harrington R a. The Preparation of Acetylenic Ketones Using Soluble Silver Acetylides. J Am Chem Soc. 1956; 78:1675–1678.

28. Naka T, Koide K. A novel and simple method to prepare g-hydroxy-a, b-(E) -alkenoic esters from g-keto-alkynoic esters. Tetrahedron Lett. 2003; 44:443–445.

29. Wei C, Li Z, Li CJ. The First Silver-Catalyzed Three-Component Coupling of Aldehyde, Alkyne, and Amine. Org Lett. 2003; 5:4473–4475.

30. Orsini A, Vitérisi A, Bodlenner A, Weibel JM, Pale P. A chemoselective deprotection of trimethylsilyl acetylenes catalyzed by silver salts. Tetrahedron Lett. 2005; 46:2259–2262.

31. Zheng W, Stasch A, Prust J, et al. Anion-templated syntheses of rhombohedral silver-Alkynyl cage compounds. Angew Chem Int Ed. 2001; 40:3464–3467.

32. Qiao J, Shi K, Wang QM. A giant silver alkynyl cage with sixty silver(I) ions clustered around polyoxometalate templates. Angew Chem Int Ed. 2010; 49:1765–1767.

33. Shi L, Jing C, Ma W, et al. Plasmon resonance scattering spectroscopy at the single-nanoparticle level: real-time monitoring of a click reaction. Angew Chem Int Ed. 2013; 52:6011–4.

34. Chumbimuni-Torres KY, Dai Z, Rubinova N, et al. Potentiometric biosensing of proteins with ultrasensitive ion-selective microelectrodes and nanoparticle labels. J Am Chem Soc. 2006; 128:13676–13677.

35. Wang J, Polsky R, Xu D. Silver-enhanced colloidal gold electrochemical stripping detection of DNA hybridization. Langmuir. 2001; 17:5739–5741.